

**Supplementary information for
Integrative analysis reveals early epigenetic alterations in high-grade serous
ovarian carcinomas**

Hidenori Machino, Ai Dozen, Mariko Konaka, Masaaki Komatsu, Kohei Nakamura,
Noriko Ikawa, Kanto Shozu, Ken Asada, Syuzo Kaneko, Hiroshi Yoshida, Tomoyuki
Kato, Kentaro Nakayama, Vassiliki Saloura, Satoru Kyo, and Ryuji Hamamoto

The file contains

Supplementary Tables 1 – 2

Supplementary Figures 1 – 7

Supplementary Table 1 Information of certified cell lines.

Name	Certification institution	<i>BRCA1</i>	<i>BRCA2</i>	Tested method	DNA profile or characteristics
293T	ATCC	Not assessed	Not assessed	STR	Amelogenin: X CSF1PO: 11, 12 D13S317: 12, 14 D16S539: 9, 13 D5S818: 8, 9 D7S820: 11 THO1: 7, 9.3 TPOX: 11 vWA: 16, 19
CaOV3	ATCC	Wild type	Wild type	STR	Amelogenin: X CSF1PO: 10, 13 D13S317: 12 D16S539: 9 D5S818: 12 D7S820: 10 THO1: 7 TPOX: 8, 10 vWA: 16, 18
ES2	ATCC	Wild type	Wild type	STR	Amelogenin: X CSF1PO: 10 D13S317: 11 D16S539: 11, 13 D5S818: 11, 13 D7S820: 11 THO1: 9.3 TPOX: 8, 12 vWA: 16, 17
JHOS-2	RIKEN CELL BANK	M1? (Driver)	Wild type	STR	Amelogenin: X CSF1PO: 11 D13S317: 8, 9 D16S539: 13 D21S11: 31, 31.2 D5S818: 10 D7S820: 11 THO1: 6, 7 TPOX: 8, 11 vWA: 14, 17
JHOS-4	RIKEN CELL BANK	Y1202Qfs *12 (Driver)	Wild type	STR	Amelogenin: X CSF1PO: 10 D13S317: 11 D16S539: 9, 10 D21S11: 29, 31.2 D5S818: 11 D7S820: 10 THO1: 7 TPOX: 8, 12 vWA: 14
OVCAR3	RIKEN CELL BANK	Wild type	HOMDEL (Driver)	STR	Amelogenin: X CSF1PO: 11, 12 D13S317: 12 D16S539: 12 D5S818: 11, 12 D7S820: 10 THO1: 9, 9.3 TPOX: 8 vWA: 17
KURAMOCHI	JCRB	HOMDEL (Driver)	R2318* (Driver)	STR	Amelogenin: X CSF1PO: 11, 12 D13S317: 9, 12 D16S539: 10 D5S818: 12 D7S820: 10, 11 THO1: 9 TPOX: 8, 12 vWA: 16, 19
OVSAHO	JCRB	Wild type	HOMDEL (Driver)	STR	Amelogenin: X CSF1PO: 10, 12 D13S317: 8 D16S539: 9 D5S818: 12, 13 D7S820: 8, 10 THO1: 6 TPOX: 8, 11 vWA: 14
RMUGS	JCRB	Wild type	Wild type	STR	Amelogenin: X CSF1PO: 12 D13S317: 10, 11 D16S539: 10, 11 D5S818: 10, 14 D7S820: 12 THO1: 9 TPOX: 8, 11 vWA: 14, 16
TYK-nu	JCRB	Wild type	Wild type	STR	Amelogenin: X CSF1PO: 12 D13S317: 10, 11 D16S539: 9, 10 D5S818: 12, 13 D7S820: 10 THO1: 9 TPOX: 9, 11 vWA: 14, 16
SNU8	KCLB	Wild type	Wild type	STR	Amelogenin: X CSF1PO: 9, 12 D13S317: 8, 9 D3S1358: 14, 16 D5S818: 11, 12 D7S820: 8, 12 FGA: 20, 26 THO1: 7, 9 TPOX: 11 vWA: 17

ATCC; American Type Culture Collection

JCRB; Japanese Collection of Research Bioresources

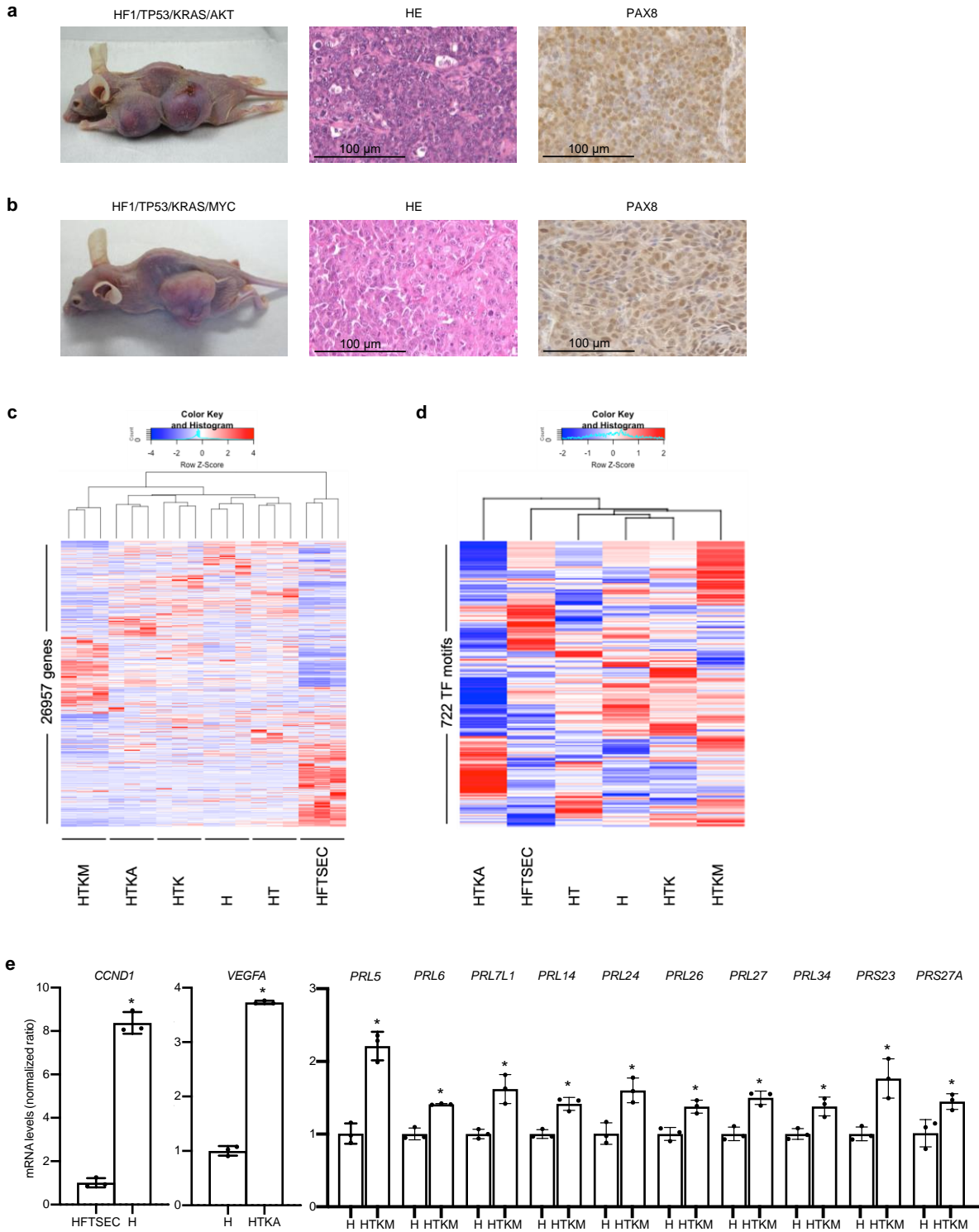
KCLB; Korean Cell Line Bank

BRCA1 and *BRCA2* gene profiles were sourced from Cancer Cell Line Encyclopedia (CCLE).

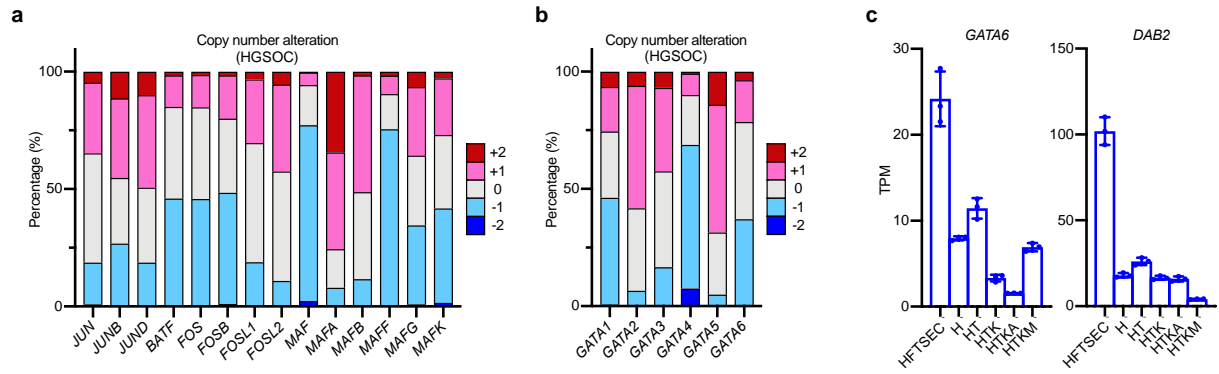
Supplementary Table 2 Information of primers.

Primer names	Purpose	Direction	Sequence (5' -> 3' direction)
<i>GAPDH</i>	qPCR	Forward	GCAAATTCCATGGCACCGTC
		Reverse	TCGCCCACTTGATTTTGG
<i>MAF</i>	qPCR	Forward	TATGCCCAGTCTGCCGCTT
		Reverse	CGCTGCTCGAGCCGTTTTCT
<i>GATA6</i>	qPCR	Forward	GCCACTACCTGTGCAACGCCT
		Reverse	CAATCCAAGCCGCCGTGATGAA
<i>DAB2</i>	qPCR	Forward	CTCTGTCCAGTCCTCACCACAT
		Reverse	GTTCTGAGACGGGAGGAGCAAA
<i>WWOX</i>	qPCR	Forward	TCCTCCAGGATGTTTTGTGCCG
		Reverse	AAGCCAGCATCGCCCAATAGTC
<i>CDH1</i>	qPCR	Forward	GCCTCCTGAAAAGAGAGTGGAAG
		Reverse	TGGCAGTGTCTCTCCAAATCCG
<i>DANCR</i>	qPCR	Forward	GCCACTATGTAGCGGGTTTC
		Reverse	ACCTGCGCTAAGAAGTGGG
<i>CXCL1</i>	qPCR	Forward	AGCTTGCCTCAATCCTGCATCC
		Reverse	TCCTTCAGGAACAGCCACCAGT
<i>CXCL2</i>	qPCR	Forward	AGGGGTTGCGCGTTCTCGGA
		Reverse	CCGCAGGAGCCGGGGATTG
<i>CXCL3</i>	qPCR	Forward	CGCCCAAACCGAAGTCATAG
		Reverse	GCTCCCCTTGTTCAGTATCTTTT
<i>CXCL5</i>	qPCR	Forward	GAGAGCTGCGTTGCGTTTGTTTAC
		Reverse	CCGTTCTTCAGGGAGGCTACCACT
<i>CXCL8</i>	qPCR	Forward	CACTGCGCCAACACAGAAAT
		Reverse	GCCCTCTTCAAAAAGTCTCCAC
<i>PSMB8</i>	qPCR	Forward	CCTTACCTGCTTGGCACCATGT
		Reverse	TTGGAGGCTGCCGACACTGAAA
<i>PSMB9</i>	qPCR	Forward	CGAGAGGACTTGTCTGCACATC
		Reverse	CACCAATGGCAAAGGCTGTGCG
<i>CCND1</i>	qPCR	Forward	CTGGCCATGAACTACCTGGA
		Reverse	GTCACACTTGATCACTCTGG
<i>VEGFA</i>	qPCR	Forward	CAAGACAAGAAAATCCCTGTGG
		Reverse	GCTTGTCACATCTGCAAGTACG
<i>RPL5</i>	qPCR	Forward	CCAAATACAGGATGATAGTTCGTG
		Reverse	TTGGCAGTTCGTGTGCATACGC
<i>RPL6</i>	qPCR	Forward	CCTTGTCAGAGGAATTGGCAGG
		Reverse	GTAACAGTTGCGAGAACCTTCTC
<i>RPL7L1</i>	qPCR	Forward	TGACAAGGTGCGTCTCAGACGA
		Reverse	TCTGCACCAGTAAACTCACGCC
<i>RPL14</i>	qPCR	Forward	GCCGCGAGTAAAAAGGCTCCAG
		Reverse	TGCCTTTGGAGCAGGTGCTTTC
<i>RPL24</i>	qPCR	Forward	CTCGGCAGATAAACTGGACTGTC
		Reverse	GCAAGAGATGCACCAGTAATGGC
<i>RPL26</i>	qPCR	Forward	GGCTAATGGCACAAGTGTCCAC
		Reverse	GGCGAGATTTGGCTTTCCGTTT
<i>RPL27</i>	qPCR	Forward	TGGACAAAAGTGTGCTCAATAAGG
		Reverse	AGAACCACTTGTTCTTGCCGTGC
<i>RPL34</i>	qPCR	Forward	GACCTAAAGTTCTTATGAGATTGTC
		Reverse	CTGACTCTGTGCTTGTGCCTTC

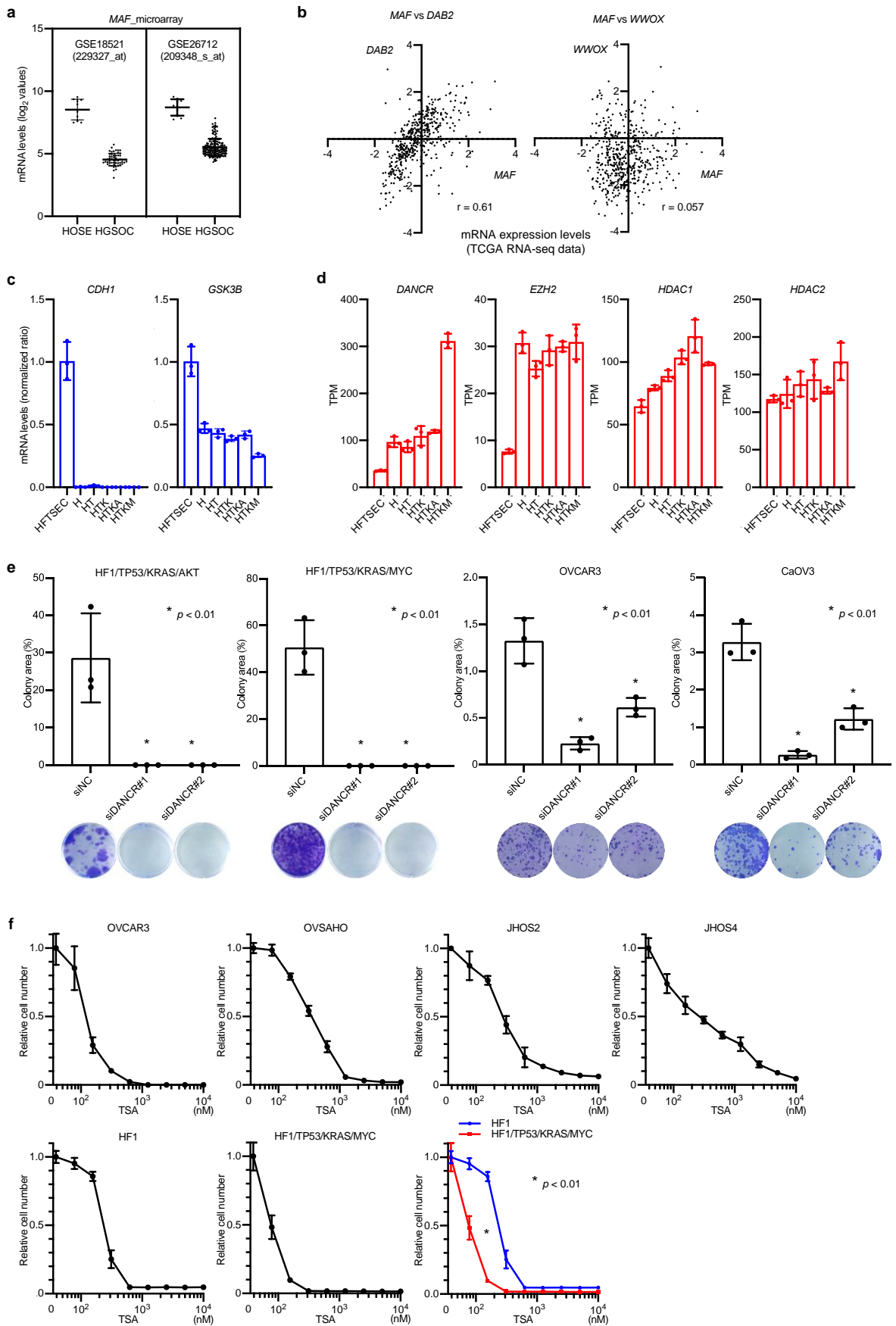
<i>RPS23</i>	qPCR	Forward	AGGAAGTGTGTAAGGGTCCAGC
		Reverse	CACCAACAGCATGACCTTTGCG
<i>RPS27A</i>	qPCR	Forward	GCAGAGACTGATCTTTGCTGGC
		Reverse	CTTGGGAGTGGTGTAAAGACTTCT
<i>SNAI1</i>	qPCR	Forward	TGCCCTCAAGATGCACATCCGA
		Reverse	GGGACAGGAGAAGGGCTTCTC
<i>COL4A1</i>	qPCR	Forward	TGTTGACGGCTTACCTGGAGAC
		Reverse	GGTAGACCAACTCCAGGCTCTC
<i>CRB3</i>	qPCR	Forward	CTTCTGCAAATGAGAATAGCACTG
		Reverse	GACCACGATGATAGCAGTGATGG
<i>DSP</i>	qPCR	Forward	TGACAGACCGCTGGCAAAGGAT
		Reverse	GGCGTTTAGCATCATAGAGCCAC
<i>MUC1</i>	qPCR	Forward	CCTACCATCCTATGAGCGAGTAC
		Reverse	GCTGGGTTTGTGTAAGAGAGGC
<i>OCN</i>	qPCR	Forward	ATGGCAAAGTGAATGACAAGCGG
		Reverse	CTGTAACGAGGCTGCCTGAAGT
<i>GSK3B</i>	qPCR	Forward	CCGACTAACACCACTGGAAGCT
		Reverse	AGGATGGTAGCCAGAGGTGGAT



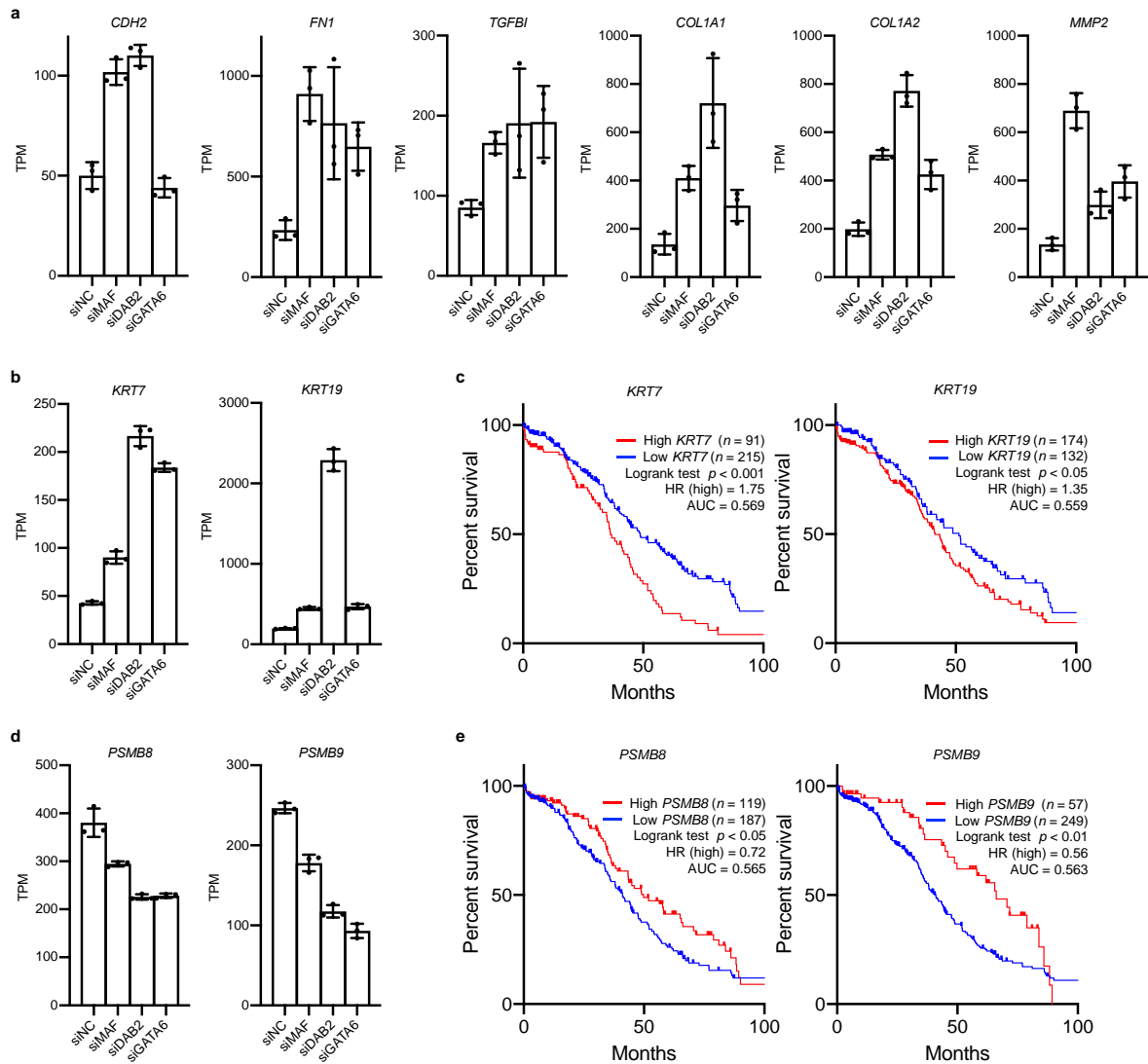
Supplementary Fig. 1 Mouse xenograft experiments and integrative analysis of stepwise HGSOc model cells. **a–b** Subcutaneous mouse xenograft experiments using HF1/TP53/KRAS/AKT (a) and HF1/TP53/KRAS/MYC (b) cells, respectively. The confirmation of the HGSOc-like phenotype in the mouse xenograft experiments was carried out by a pathologist who examined the results of hematoxylin eosin (HE) staining and PAX8 staining, which is a positive marker for HGSOc. Scale bars, 100 μ m. Detailed information of mouse xenograft experiments is previously described¹¹. **c** A heatmap with hierarchical clustering of gene expression levels calculated using RNA-seq. **d** A heatmap with hierarchical clustering of TF motif enrichment scores calculated using ATAC-seq. **e** mRNA expression levels (RT-qPCR; n = 3) of *CCND1*, *VEGFA*, and ribosomal protein genes in the indicated HGSOc model cells. Error bars represent mean \pm standard deviation (SD). Statistical analysis was performed using unpaired Student's t-test. * $p < 0.05$.



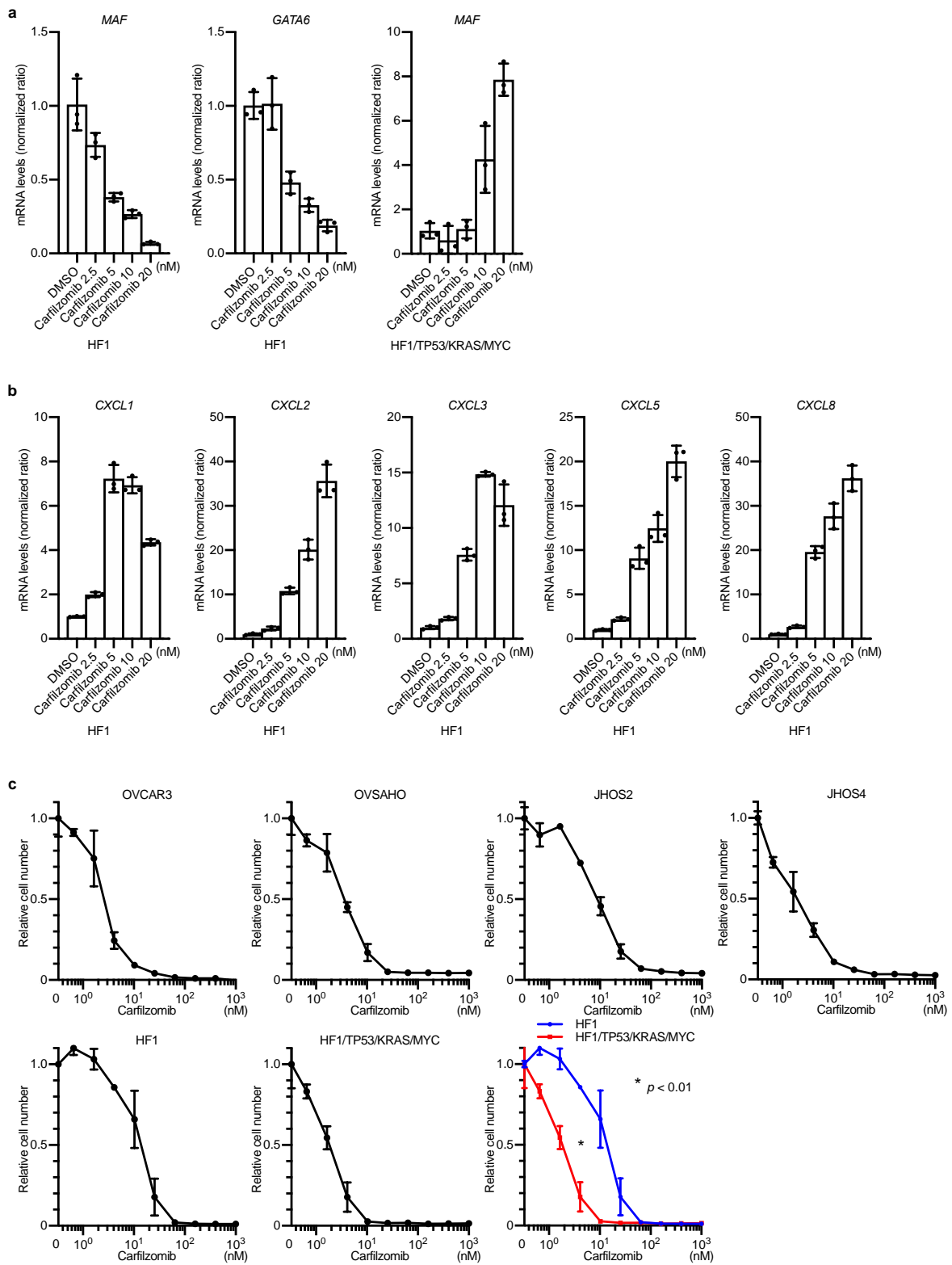
Supplementary Fig. 2 AP-1 family and GATA family genes are dysregulated in HGSOCS. **a–b** Copy number alteration (CNA) of AP-1 family genes (a) and GATA family genes (b) in HGSOCS samples. Each sample was segregated according to their CNA status: amplification (CNA = +2); gain (CNA = +1); duplicate (CNA = 0); deletion (CNA = -1); deep deletion (CNA = -2). Data are sourced from TCGA project of HGSOCS. **c** mRNA expression levels (RNA-seq, n = 3) of *GATA6* and *DAB2* are downregulated in HGSOCS model cells. Error bars represent mean \pm standard deviation (SD).



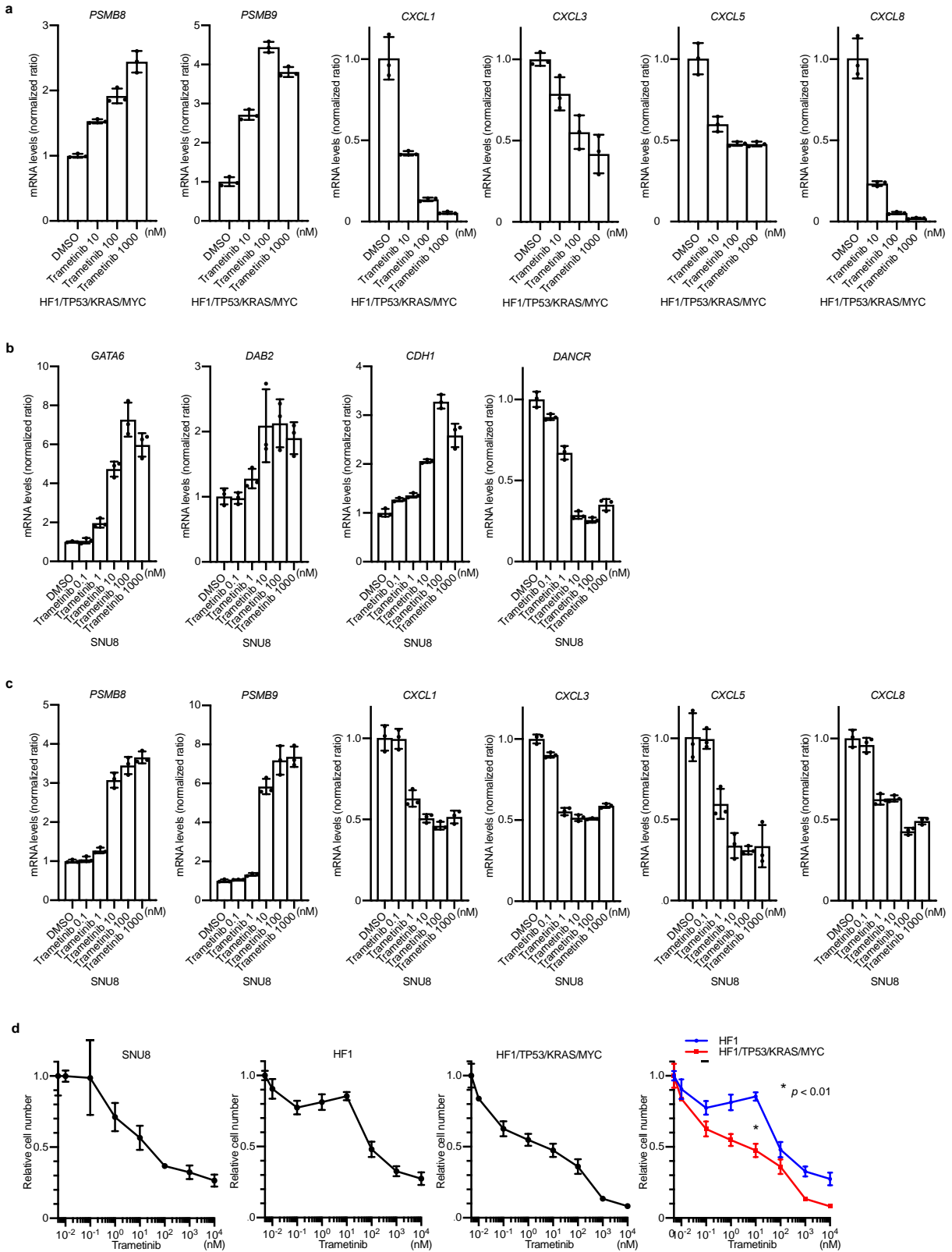
Supplementary Fig. 3 Integrative analysis identifies targetable genes in HGSOCS. **a** mRNA expression levels of *MAF* in two independent microarray datasets. GSE18521 and GSE26712 contain microarray data of human ovarian surface epithelial cell (HOSE) samples and HGSOC samples [GSE18521(HOSE: n = 10, HGSOC: n = 53) and GSE26712 (HOSE: n = 10, HGSOC: n = 185)]. Statistical analysis was performed using unpaired Student's t-test. Error bars represent mean \pm standard deviation (SD). **b** mRNA expression levels of *MAF* are plotted against those of *DAB2* and *WWOX* (n = 489). The data were analyzed using Pearson's correlation coefficients. **c** mRNA expression levels (RT-qPCR, n = 3) of epithelial-mesenchymal transition (EMT)-related genes. Downregulation of epithelial markers, including *CDH1* and *GSK3B*, are observed during oncogenic transformation. Error bars represent mean \pm standard deviation (SD). **d** mRNA expression levels (RNA-seq, n = 3) of *DANCR*, *EZH2*, *HDAC1* and *HDAC2* are upregulated in HGSOC model cells. Error bars represent mean \pm SD. **e** Colony formation assay with *DANCR* siRNA knockdown experiments in HF1/TP53/KRAS/AKT, HF1/TP53/KRAS/MYC, OVCAR3, and CaOV3 cells. Error bars represent mean \pm SD of three biological replicates. Statistical analysis was performed using unpaired Student's t-test. **f** Cell viability assay with TSA treatment. The cytotoxic effects of TSA are amplified in tumorigenic HGSOC model cells. Relative cell number shows the relative ratio between the number of cells in the absence of the inhibitors and the number of cells in the presence of various concentrations of TSA. Error bars represent mean \pm SD of three biological replicates.



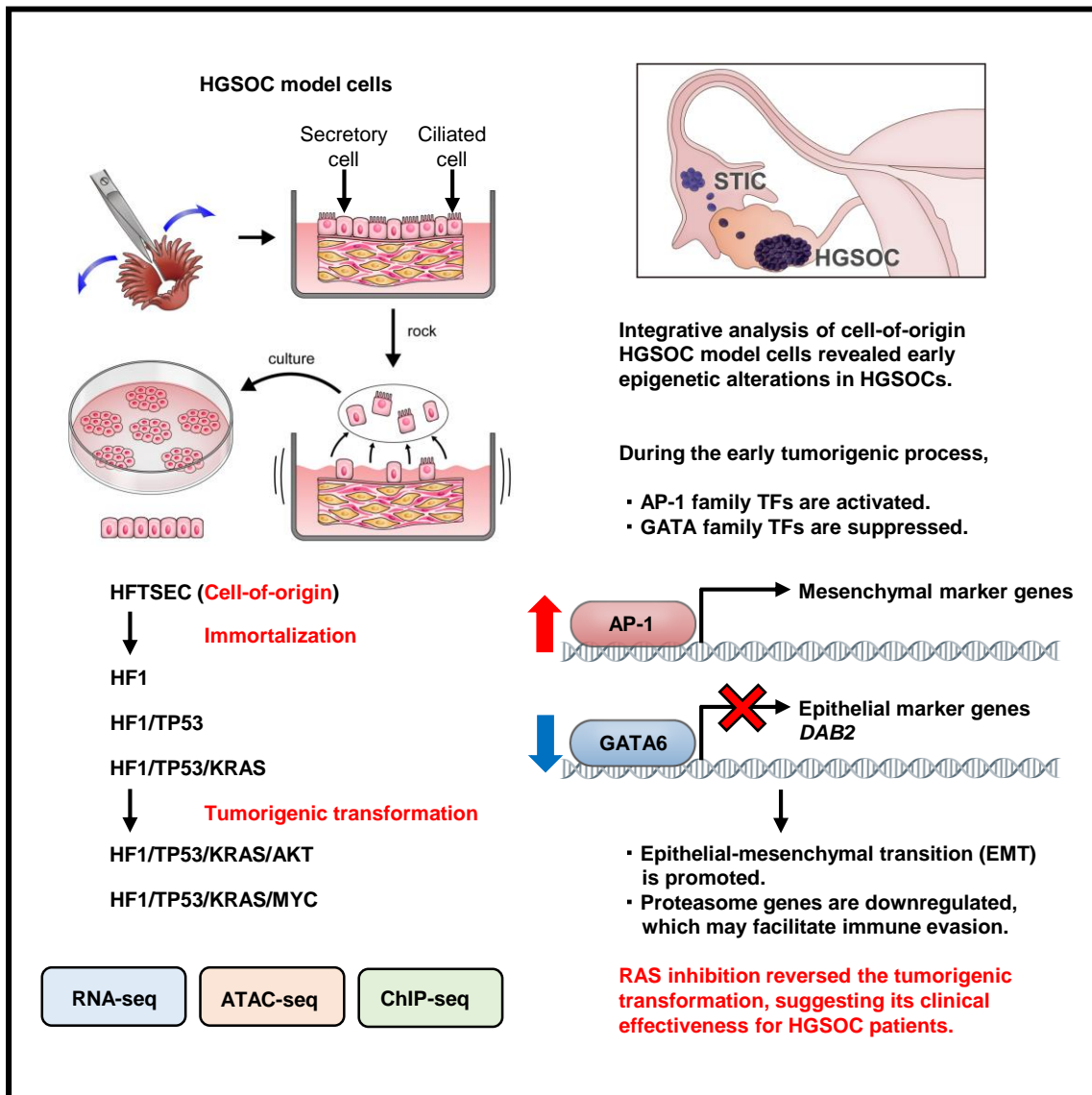
Supplementary Fig. 4 Inhibition of *MAF*, *GATA6* and *DAB2* upregulates epithelial-mesenchymal transition (EMT)-related genes and poor prognostic genes of HGSCs. **a** mRNA expression levels (RNA-seq; n = 3) of EMT-related genes upon siRNA knockdown of *MAF*, *GATA6* and *DAB2* in HF1 cells. Inhibition of *MAF*, *GATA6* and *DAB2* upregulates EMT-related genes. Error bars represent mean \pm standard deviation (SD). **b** mRNA expression levels (RNA-seq; n = 3) of *KRT7* and *KRT19* genes upon siRNA knockdown of *MAF*, *GATA6* and *DAB2* in HF1 cells. Error bars represent mean \pm SD. **c** Kaplan-Meier survival curves classified by high or low *KRT7* or *KRT19* mRNA expression levels in the TCGA HGSC cohort. High *KRT7* and high *KRT19* group exhibits poor overall survival. **d** mRNA expression levels (RNA-seq; n = 3) of *PSMB8* and *PSMB9* genes upon siRNA knockdown of *MAF*, *GATA6* and *DAB2* in HF1 cells. Error bars represent mean \pm SD. **e** Kaplan-Meier survival curves classified by high or low *PSMB8* or *PSMB9* mRNA expression levels in the TCGA HGSC cohort. Low *PSMB8* and Low *PSMB9* group exhibits poor overall survival.



Supplementary Fig. 5 A proteasome inhibitor causes both of early oncogenic alterations and tumor suppressive effects. **a** mRNA expression levels (RT-qPCR; n = 3) of *MAF*, *GATA6* upon carfilzomib treatment in HF1 and HF1/TP53/KRAS/MYC cells. Inhibition of proteasome imitate the early oncogenic alterations of *MAF* and *GATA6* downregulation in HF1 cells, whereas it recovers *MAF* expression in HF1/TP53/KRAS/MYC cells. Error bars represent mean \pm standard deviation (SD). **b** mRNA expression levels (RT-qPCR; n = 3) of chemokine genes are upregulated upon carfilzomib treatment in HF1 cells. Error bars represent mean \pm SD. **c** Cell viability assay with carfilzomib treatment. The cytotoxic effects of carfilzomib are amplified in HGSOc model cells. Relative cell number shows the relative ratio between the number of cells in the absence of the inhibitors and the number of cells in the presence of various concentrations of carfilzomib. Error bars represent mean \pm SD of three biological replicates.



Supplementary Fig. 6 A MEK inhibitor reverses early oncogenic alterations in HGSOCs. a mRNA expression levels (RT-qPCR; n = 3) of immunoproteasome and chemokine genes upon trametinib treatment in HF1/TP53/KRAS/MYC cells. Error bars represent mean \pm standard deviation (SD). **b,c** mRNA expression levels (RT-qPCR; n = 3) of dysregulated genes in HGSOCs are recovered upon carfilzomib treatment in SNU8 cells. Error bars represent mean \pm SD. **d** Cell viability assay with trametinib treatment. The cytotoxic effects of trametinib are amplified in HGSOC model cells. Relative cell number shows the relative ratio between the number of cells in the absence of the inhibitors and the number of cells in the presence of various concentrations of carfilzomib. Error bars represent mean \pm SD of three biological replicates.



Supplementary Fig. 7 A graphical summary of the present study.